

# COUPLING TURBULENCE IN HYBRID LES-RANS TECHNIQUES

**Stephen Woodruff**

Computational AeroSciences Branch,  
NASA Langley Research Center,  
Hampton, VA 23681  
stephen.l.woodruff@nasa.gov

## ABSTRACT

A formulation is proposed for hybrid LES-RANS computations that permits accurate computations during resolution changes, so that resolution may be changed at will in order to employ only as much resolution in each subdomain as is required by the physics. The two components of this formulation, establishing the accuracy of a hybrid model at constant resolutions throughout the RANS-to-LES range and maintaining that accuracy when resolution is varied, are demonstrated for decaying, homogeneous, isotropic turbulence.

## INTRODUCTION

Advances in computing power have made hybrid Large-Eddy Simulation (LES) - Reynolds-Averaged Navier-Stokes (RANS) approaches feasible for practical problems where RANS methods alone yield unsatisfactory results or do not provide necessary time-dependent information. These methods have been most successful when the flow is dominated by rapid production of turbulence in the free shear layers and there is little interaction between the turbulence of the wall-bounded and free-shear layers (Travin et al., 1999).

In order for the full potential of hybrid computations to be realized, the turbulence in the RANS and LES regions must be coupled. Efforts to do this have met with some success in certain situations (such as Davidson and Billson, 2006; Keating et al., 2006; Shur et al., 2008; Choi et al., 2009; Hamba, 2009), but there exists as yet no proven general procedure for a fully coupled hybrid computation which permits LES-RANS transitions to be set according to the physics of the problem rather than the requirements of the modelling technique. Hamba's (2009,2011) work points to the need to add correction terms to the governing equations, as advocated here.

A related question is whether RANS and LES models may be extended to model the full range of resolutions between that of RANS and that of LES (Speziale, 1998; Woodruff et al., 2000; Girimaji and Abdol-Hamid, 2005). The resulting *continuous models* would clearly be advantageous for hybrid methods, not least because one could make RANS-LES transitions gradually, without sacrificing physical fidelity.

Here, a formulation which addresses these questions is

presented. Its ultimate goal is to provide a modelling capability where each portion of the flow is solved only with the resolution required by the fluid mechanics and where transitions between regions of different resolution are free of unphysical artifacts.

Decaying, homogeneous, isotropic turbulence is employed as a test case. The flow is solved with a spectral code and the Detached-Eddy Simulation formulation of Strelets (2001) is used as a representative hybrid modelling technique.

To investigate the potential for successful modelling in the range of resolutions between RANS and LES, several model coefficients were assumed to be functions of the spectral-code resolution,  $N$ , and a simple gradient-based optimization scheme was employed to determine model-constant values at each of several resolutions. The optimization scheme sought to minimize the difference between the temporal evolution of the total kinetic energy as determined by the low-resolution simulation and the same quantity as determined from a full-scale LES.

The basic problem with moving between regions of different resolutions is that flow variables change as a result of the change in resolution. This change in the flow variables is in addition to that due to the modelled and resolved physics of the flow. For example, the modelled turbulent kinetic energy increases while the kinetic energy of the resolved motion decreases when the resolution is decreased. If left to its own devices, the simulation will only gradually adapt as the resolution changes and unphysical behavior will result. To avoid this, resolution-dependent source terms are added to the governing equations; these correction terms employ the resolution gradient and the variations of the flow quantities with resolution to counteract the non-physical effects of changes in resolution. The effectiveness of this procedure is demonstrated by performing a successful decaying, homogeneous, isotropic turbulence computation with temporally and spatially varying resolution.

The two parts of the hybrid formulation, establishing the accuracy of a hybrid model through a range of constant resolutions and establishing that the accuracy is retained when the resolution is made variable, are described in the next section. The numerical test case for these ideas is presented in the following section and then two sections address demonstrations

of the formulation’s two parts. The final section presents conclusions.

## OUTLINE OF HYBRID FORMULATION

It is not difficult to formulate decompositions for the velocity and the other flow variables that yield various mixtures of RANS and LES as some parameter, a “blending parameter”, is varied. A combined space and time filter, for example, could be constructed so that the time constant is very long for RANS, but very short for LES; the spatial filter width would vary with resolution as is typical for LES. The blending parameter has some (possibly implicit) relationship with the resolution, since a more RANS-like mixture would be appropriate for a coarser resolution and a more LES-like mixture would be appropriate for a finer resolution.

Unfortunately, it is very difficult to take the next step of deriving a turbulence model that corresponds to a specific decomposition of the flow variables. In the present formulation, the process is reversed: a hybrid model and governing equations are selected and the decomposition of the flow variables is that which results when these equations are solved. The question is then what properties the model and equations must have so that a useful hybrid computation results.

The goal of coupling the turbulent part of the flow in regions with different resolutions — and thus different mixtures of resolved and modelled turbulence — is to be achieved by changing resolution continuously, with the accuracy of mean- and turbulent-flow predictions maintained throughout the transition. This requirement of maintaining accuracy throughout the transition may be met by imposing two requirements on the hybrid model and equations: that the model yield accurate predictions at fixed resolutions throughout the RANS-to-LES range and that this accuracy be maintained across spatial or temporal resolution changes in a given computation.

Before considering how to impose these requirements, it is necessary to understand precisely how accuracy is to be evaluated in a hybrid computation. This is an issue because the dependent variables in the equations will naturally depend on the blending parameter in the hybrid model, but this parameter, as an artifact of the model, should have no effect on physically meaningful outputs of the computation. The concept of model-invariant quantities is introduced to address this issue: a model-invariant quantity is a dependent variable or combination of dependent variables that is (at least approximately) independent of the model blending parameter. Model-invariant quantities thus represent physically meaningful results and may be used to evaluate the accuracy of a hybrid computation.

One type of model-invariant quantity is represented by the mean-flow variables, because for RANS, or for LES, or for any combination of the two, an average of the resolved flow variables is defined that corresponds to the physical mean quantity. A second type of model-invariant quantity involves a combination of resolved and modelled flow variables, with information shifting from the resolved part to the modelled part and back as the model blending parameter varies. The primary example of such a quantity in a hybrid LES-RANS computation is the stress tensor, which is comprised of a resolved contribution, a modelled contribution and, potentially,

contributions from cross terms, etc. Of particular importance is the turbulent kinetic energy, the trace of this tensor.

It will be assumed in the present work that the hybrid model has been constructed so that model-invariant quantities are at least approximately invariant. In the following, it will be seen that the model-invariance accuracy may be improved through the use of resolution-dependent coefficients in the turbulence model. It will also be seen that the requirement that model invariance be preserved when the resolution changes provides important insights into the nature of a hybrid formulation. The shear-stress relation of Germano (1992) is based on a similar observation.

As mentioned in the introduction, continuous models (models that are accurate throughout the RANS-to-LES range of resolutions) have been proposed in several forms. In the present work, a continuous model is sought which has the structure of the Strelets (2001) hybrid model, but has resolution-dependent model coefficients. The use of a systematic optimization approach for determining the model coefficients as a function of resolution is described in the following section.

Having established the accuracy of the continuous model for constant resolutions in the range between that of LES and that of RANS, it remains to determine if that accuracy may be maintained when the resolution varies spatially or temporally in a given computation. Since validation of the continuous model (for constant resolutions) consisted of comparing model-invariant quantities with some reference computation or experiment, maintaining accuracy when the resolution varies is possible only if model invariance is preserved when the resolution becomes spatially or temporally variable. It will now be shown that the variable resolution must be introduced in a particular way in order to preserve model invariance and, even more fundamentally, to avoid altering the physical balances in the governing equations.

Consider a typical flow variable in a computation where the resolution is constant, such as a velocity component  $u = u(t', \mathbf{x}', \Delta_0)$ . It is a function of time,  $t'$ , space,  $\mathbf{x}'$ , and of the constant model blending parameter  $\Delta_0$ . (For simplicity, the blending parameter is taken here to be simply the resolution, but the same analysis applies to more sophisticated measures of the RANS-LES mixture, such as the ratio of turbulence length scale to local grid resolution.) The standard means of introducing variable resolution into the formulation (Spalart, 2009) is by replacing the constant blending parameter  $\Delta_0$  in the hybrid model with a variable parameter  $\Delta = \Delta(t', \mathbf{x}')$ . The value of a flow variable like  $u$  at any point and time now depends on the whole function  $\Delta(t', \mathbf{x}')$  (that is, the values of  $\Delta$  at all positions and all previous times). It is convenient to make the fairly drastic assumption that  $u$  depends only on the local value of  $\Delta$ :  $u = u(t', \mathbf{x}', \Delta(t', \mathbf{x}'))$ . This assumption is already made in most LES turbulence models, where the eddy viscosity is constructed using only the local value of the grid resolution, so no additional approximation is being made here.

Introducing the variable resolution  $\Delta$  in this way produces a new contribution to the derivatives of  $u$  that reflects the variation of  $u$  due not to physical effects, but purely to the change in the structure of the model as  $\Delta$  varies. The time derivative, for example, is now  $\frac{\partial u}{\partial t'} = u_1 + u_3 \frac{\partial \Delta}{\partial t'}$ , where  $u_1$  and  $u_3$  represent the derivatives of  $u$  with respect to its first and third arguments, respectively. Similar expressions hold

for the spatial derivatives.

These new contributions to the derivatives of the flow variables disrupt the physical balances in model-invariant quantities and in the governing equations. The modelled contribution to the stress tensor, for example, contains velocity derivatives (in the Boussinesq approximation); if model-invariance holds in the constant- $\Delta$  case, it can't hold in the variable- $\Delta$  case due to the variation in  $\Delta$  contained in the new contributions to the velocity derivatives. Even if the Boussinesq approximation is not employed, some form of gradient-based model-invariant quantity will be required to validate the model fully, and this quantity will fail to be model invariant for the same reason. The governing equations are also affected, as they represent balances between physical quantities involving spatial and temporal derivatives. The contributions to the derivatives due to changes in the model structure disturb these balances, too, and spurious, non-physical, effects are seen in the solutions as a result.

This is all avoided in the present formulation by means of a simple coordinate transformation between the constant- $\Delta$  and variable- $\Delta$  cases which guarantees that properties of the constant- $\Delta$  case are mapped onto corresponding properties of the variable- $\Delta$  case. In particular, model-invariant quantities are guaranteed to transform into model-invariant quantities, and the requirement that accuracy be maintained as resolution varies is satisfied.

The transformation takes the form  $t = t'$ ,  $\mathbf{x} = \mathbf{x}'$  and  $s = \Delta_0 - \Delta(t', \mathbf{x}')$ . The variable  $s$  in the unprimed coordinate system corresponds to  $\Delta_0$  in the primed system. It provides an unambiguous means of referring to variations due to model structure now that the blending parameter is a function of space and time.

Under this transformation, the flow variable  $u$  becomes  $u = u(t, \mathbf{x}, \Delta(t, \mathbf{x}) + s)$  and the physical solution corresponds to the surface  $s = 0$ . This is, so far, essentially the same as the standard formulation described above; where it differs is in the treatment of derivatives in model-invariant quantities, in the governing equations and anywhere else. The derivatives must conform to the coordinate transformation and so the time derivative becomes

$$\frac{\partial}{\partial t'} = \tilde{\partial}_t \equiv \frac{\partial}{\partial t} - \frac{\partial \Delta}{\partial t} \frac{\partial}{\partial s} \quad (1)$$

the gradient operator becomes

$$\nabla' = \tilde{\nabla} \equiv \nabla - (\nabla \Delta) \frac{\partial}{\partial s} \quad (2)$$

( $\nabla'$  is the gradient operator on the primed variables) and the divergence of a vector  $\mathbf{v}$  becomes

$$\nabla' \cdot \mathbf{v} = \tilde{\nabla} \cdot \mathbf{v} \equiv \nabla \cdot \mathbf{v} - (\nabla \Delta) \cdot \frac{\partial \mathbf{v}}{\partial s} \quad (3)$$

(The work of Hamba (2009,2011), involving a spatially-varying filtering operation, introduces similar derivatives.)

The new terms introduced by the transformation of the derivatives have the effect of cancelling the spurious derivative contributions due to the variable blending parameter,

yielding expressions that reflect the true, physical, derivatives. This means,  $\tilde{\partial}_t$ , not  $\frac{\partial}{\partial t}$ , should be understood as the physical time derivative,  $\tilde{\nabla}$  should be understood as the physical gradient operator, etc. The procedure for transforming governing equations, model-invariant quantities and other expressions in their original form (in terms of what are here denoted as primed variables) into a form appropriate for a hybrid computation (in terms of the unprimed variables) is thus to replace  $\Delta$  by  $\Delta + s$ , the time derivative by  $\tilde{\partial}_t$ , the gradient operator by  $\tilde{\nabla}$  and so on.

Derivatives with respect to  $\Delta_0$  transform to derivatives with respect to  $s$ , which means the relation  $\frac{\partial F}{\partial \Delta_0} = 0$ , reflecting the model invariance of a quantity  $F$  in the constant- $\Delta$  case, transforms to the relation  $\frac{\partial F}{\partial s} = 0$ , expressing the model invariance of  $F$  in the variable- $\Delta$  case. This is the formal demonstration that the present formulation preserves model invariance and thus accuracy is preserved across changes in resolution.

The presence of derivatives with respect to  $s$  in the new expressions for the physical derivatives means that the new variable  $s$  is not simply a parameter. The governing equations become partial differential equations in the variables  $t$ ,  $\mathbf{x}$  and  $s$ , with appropriate initial and boundary conditions. These equations must be solved, and the result evaluated at  $s = 0$ , to arrive at the physical solution.

In the present computation, several simultaneous computations are run with  $\Delta$  offset by slightly different amounts and the  $s$  derivatives are determined by finite differencing. This is equivalent to seeking a solution to the equations as a Taylor series in  $s$  near  $s = 0$ . Because the mathematical problem poses boundary values for  $s$  rather than initial values, an exact Taylor series expansion is not possible and the present approximation amounts to assuming higher-order  $s$  derivatives are small and may be neglected. This approach yields good results for the present test problem, provided the variation in resolution is not too great.

This is one of a number of promising approximations for determining the  $s$  derivatives, each with its own accuracy characteristics and computational cost. In this case, the accuracy of the approximation seems to be limited to smaller variations in resolution and the cost is two additional simultaneous simulations (yielding the total of three points in the  $s$  direction required to compute first and second derivatives by finite differences). Other approximations, with significantly better accuracy and cost characteristics, are explored in Woodruff (2011).

The remainder of the paper is devoted to demonstrating, for the case of decaying, homogeneous, isotropic turbulence, that the two parts of this formulation are achievable: accurate simulations for constant resolutions throughout the LES-to-RANS range are possible, and employing equations transformed according to the above prescription does allow the accuracy of the constant-resolution computations to be maintained in the variable-resolution case.

## TEST PROBLEM AND NUMERICS

The test problem chosen for this initial investigation is decaying homogeneous, isotropic turbulence. While the relative simplicity of this flow makes it prone to idiosyncratic behavior (more dependence on initial conditions than is typi-

cal for turbulent flows, etc.), this flow provides a good, easily computable, test problem on which to begin the present study. The equations to be solved are thus the three-dimensional incompressible Navier-Stokes equations plus a turbulence model. Following the procedure of the last section, the continuity and momentum equations become

$$\begin{aligned}\tilde{\nabla} \cdot \mathbf{v} &= 0 \\ \partial_t \mathbf{v} + (\mathbf{v} \cdot \tilde{\nabla}) \mathbf{v} &= -\frac{1}{\rho} \tilde{\nabla} p + \tilde{\nabla} \cdot ((\mathbf{v} + \mathbf{v}_t) \tilde{\nabla} \mathbf{v})\end{aligned}\quad (4)$$

In these equations,  $\mathbf{v}$  is the resolved-scale velocity,  $\rho$  and  $\nu$  are the constant density and molecular viscosity,  $p$  is the resolved-scale pressure, and  $\mathbf{v}_t$  is the turbulent or eddy viscosity.

The model employed in this paper is the Strelets (2001) Detached-Eddy Simulation hybrid model based on Menter's (1994) SST model,

$$\begin{aligned}\partial_t k_M + (\mathbf{v} \cdot \tilde{\nabla}) k_M &= \frac{1}{\rho} P - \frac{k_M^{3/2}}{\ell_H} + \tilde{\nabla} \cdot [(\mathbf{v} + \sigma_k \mathbf{v}_t) \tilde{\nabla} k_M] \\ \partial_t \omega_M + (\mathbf{v} \cdot \tilde{\nabla}) \omega_M &= \frac{\gamma}{\rho \nu_t} P - \beta \omega_M^2 + \tilde{\nabla} \cdot [(\mathbf{v} + \sigma_k \mathbf{v}_t) \tilde{\nabla} \omega_M] \\ &\quad + 2\sigma_\omega \frac{1}{\omega_M} \tilde{\nabla} k_M \cdot \tilde{\nabla} \omega_M\end{aligned}\quad (5)$$

The production  $P$  is expressed as  $P = \nu_t \tilde{S}_{ij} \tilde{S}_{ij}$ , where  $\tilde{S}_{ij}$  is the symmetric part of the tensor  $\tilde{\nabla} \mathbf{v}$ .

These equations describe the  $k - \varepsilon$  branch of the Menter model, active away from walls, which is the only branch of interest here. The length scale  $\ell_H$  switches between the RANS and LES length scales, and the model constants, following Menter (1994), are the standard  $k - \varepsilon$  values.

If  $\ell_M$  is regarded as representing the length scale of the large-scale, energy-containing part of the turbulent motion, then the switch from RANS to LES takes place when the grid size  $\Delta = 1/C_{DES} \ell_M \approx 1.8 \ell_M$ . That is, the switch to LES is made when the cut-off wave number is well to the left of (less than) the main energy-containing wave numbers. LES is traditionally interpreted as requiring that the cut-off wave number be to the right of the energy-containing wave numbers and well into the inertial range, so it is clear most of the job of effecting the RANS-to-LES transition falls to the LES mode of the hybrid model. For this reason, the present work will focus on the model with  $\ell_H = \ell_{LES} = C_{DES} \Delta$ . The model consequently makes the transition from pure LES to coarse LES, without taking the final step to the RANS model. It thus serves to demonstrate the effectiveness of the present formulation in dealing with the essential feature of hybrid models: their dependence on a time- and space-varying non-physical parameter. The full LES-to-RANS transition is covered in Woodruff (2011).

These equations are solved in a periodic three-dimensional box with sides of length  $2\pi$  using a pseudospectral code derived from that employed in Shebalin and Woodruff (1997). In addition to being rewritten in terms of the primitive velocity variables plus the turbulence variables  $k_M$  and  $\omega_M$ , this version of the code employs the software package *rksuite* (Brankin et al., 1992) for variable order, variable step-size, time stepping, in addition to a fixed-order, fixed

step-size scheme. While variable order- and step-size methods have been highly developed and widely used by the ODE numerical-algorithm community, they have seen limited use in turbulence computations due to the resolution demands of a given computation being relatively fixed, making the higher-overhead variable methods a poor choice. In the present investigation, however, as described below, computations are carried out over a range of parameters and it would be time consuming to determine the step size required to maintain accuracy for each set of parameters. The variable order and step-size scheme does this automatically; spot checks were performed to verify that the required accuracy was maintained.

An initial velocity field for the computation of decaying homogeneous, isotropic, turbulence was constructed by creating a uniformly distributed random velocity field and then reducing the modes within each wave-number band so the velocity spectrum is  $E(\kappa) \sim \kappa^2 \exp(-2\kappa^2/\kappa_p^2)$ , where  $\kappa_p = 13$  in the present computations. The peak in this initial spectrum is at  $\kappa = 9$ . The initial velocity field is normalized so that the total kinetic energy is unity at the initial time. The turbulence-model variables  $k_M$  and  $\omega_M$  are initialized as constants.

A  $63^3$  computation was performed with this code using the Smagorinsky model ( $C_s = 0.17$ ) for validation purposes. The initial dissipation was 1.39 and the viscosity was 0.00033, making the initial Reynolds number based on the Taylor microscale,  $Re_\lambda$ , approximately 120. The results of this computation give asymptotic behavior  $k \sim t^{-m}$ ,  $\lambda \sim t^a$ ,  $Re_\lambda \sim t^{-b}$ , with  $m \approx 1.3$ ,  $a \approx 1.0$ , and  $b \approx 0.4$ , all consistent with previous computations and measurements (Mansour and Wray, 1994), as are energy spectra at selected  $Re_\lambda$  during the decay.

In order to provide an automated and rapid means for tuning turbulence models, this code is embedded in an optimization script which generates trial values of model parameters, initiates the required simulations, compares the results with a target simulation and then generates new parameters for the next repetition. This script runs on a PBS scheduling system, providing parallelism for the optimization process. The optimization technique employed is linear dissection in each parameter; while not offering the rate of convergence of more sophisticated techniques, this approach is robust and provides thorough sampling of the parameter space.

## MODELING AT INTERMEDIATE RESOLUTIONS

To investigate the potential for successful modelling in the range of resolutions between RANS and LES, several model coefficients were assumed to be functions of the spectral-code resolution  $N$ . The optimization scheme described above was used to minimize the difference between the temporal evolution of the total kinetic energy (a model-invariant quantity) as determined by the low-resolution simulation and the same quantity as determined from the  $63^3$  validation full-scale LES mentioned in the previous section.

Determining the total kinetic energy by simply adding the resolved and modelled kinetic energies has been found to significantly over-predict the total kinetic energy in some hybrid computations (eg., Davidson and Billson, 2006). To accommodate this possibility, the total kinetic energy is constructed here as the linear combination of the resolved and modelled kinetic energy, with coefficients determined as part of the optimization process. The error is weighted to com-

pensate for the decay in the kinetic energy, so that the target kinetic energy (from the 63<sup>3</sup> validation LES) is  $O(1)$  throughout the simulation.

The initial, constant, value for the turbulent kinetic energy is chosen so that the destruction term in the kinetic energy equation,  $k_M^{3/2}/\ell_{LES}$ , equals the dissipation determined from the initial velocity field. The initial, constant, value for  $\omega_M$  and the model constant  $C_{DES}$  are determined by the optimization process.

Simulations using model constants obtained in this fashion for  $N = 8, 16, 20, 24, 28, 32$  were performed and results for the dissipation are compared in Figure 1 with that of the full-scale LES. While there is clearly room for improvement (through including more model constants in the optimization process, for example), the results are fairly good even for very low resolutions. The failure of the lower-resolution simulations to capture the slight rise in dissipation near  $t = 0.02$  is due to the model not capturing the filling-in of high-wavenumber energy bands absent from the initial spectrum. This illustrates the truism that without either accurate resolution of a flow feature or an accurate model of it, one can't hope to reproduce it.

## VARIABLE-RESOLUTION MODELING

The ability to maintain accuracy as the resolution varies in space and time is demonstrated by introducing an explicit filter into the equations and then making the filter width a function of the resolution function  $\Delta$ . Accordingly, the biharmonic operator  $C \Delta^4 \nabla^4$  was added to the right-hand side of the transport equations and the constant selected so that the total resolved kinetic energy at  $\Delta = 2\pi/20$  was approximately that of a  $20^3$  computation. The actual number of spectral modes employed in all computations of this section was  $24^3$ .

To test the ability to maintain accuracy through a temporal change in resolution, a computation was set up to begin at  $\Delta = 2\pi/20$  (resolution equivalent to  $N = 20$ ) and then change instantaneously to  $\Delta = 2\pi/18$  (resolution equivalent to  $N = 18$ ) at  $t = 3$ . The objective is for the variable-resolution computation to yield the same results at a point and time where the resolution is  $\Delta$  as a constant-resolution computation at the same  $\Delta$ . Thus, the response of the resolved kinetic energy to this ten percent decrease in resolution is compared in Figure 2 with the results from a constant  $N = 18$  resolution computation.

The ability to maintain accuracy across a spatial resolution change is demonstrated by imposing a sinusoidal variation in resolution across the computational domain in the  $y$  direction:

$$\Delta(t, x, y, z) = \frac{2\pi}{20} + h(t) \left( \frac{2\pi}{16} - \frac{2\pi}{20} \right) \left( \frac{1}{2} - \frac{1}{2} \sin(y) \right) \quad (6)$$

with a maximum resolution equivalent to  $N = 20$  at  $y = \pi/2$  and a minimum resolution equivalent to  $N = 16$  at  $y = 3\pi/2$ . The function  $h(t)$  ramps up the spatial variation: it is zero for  $t \leq 1$ , changes linearly from zero to one between  $t = 1$  and  $t = 5$  and is one for  $t \geq 5$ . This ramping is necessary so the simultaneous computations at offset resolutions can initialize

enough to provide correct  $s$  derivatives before the resolution variations begin.

Plots of the resolved kinetic energy for this computation averaged over  $x - z$  planes at  $t = 5$ , with and without the  $s$ -derivative correction terms, are compared with the corresponding plots for  $N = 20$  and  $N = 16$  computations in Figure 3. It is clear that the correction terms dramatically improve the ability of the computation to maintain the accuracy of the  $N = 20$  computation at the point ( $y = \pi/2$ ) where the resolution matches that of the  $N = 20$  computation and the accuracy of the  $N = 16$  computation at the point ( $y = 3\pi/2$ ) where the resolution matches that of the  $N = 16$  computation. This success is further demonstrated in Figure 4, where averages over the  $y = 3\pi/2$  plane are shown as functions of time for the four computations. The computation with the correction terms follows the resolution ramp reasonably well, but the uncorrected computation does poorly. The slight rises at the end of the runs are caused by the addition of the biharmonic term.

In further experiments, it was found that increasing the temporal ramp rate significantly led to reduced accuracy and, ultimately, numerical instabilities. Increasing the spatial variation significantly also led to reduced accuracy.

## CONCLUSION

The computations described in the preceding sections demonstrate that the two stages of the present hybrid formulation are feasible: First, by employing a commonly used hybrid model and allowing the coefficients to be functions of resolution, accurate results were obtained throughout the RANS-to-LES range. Second, the coordinate transformation introduced here to relate constant-resolution and variable-resolution equations permits variable-resolution computations to be carried out that maintain the accuracy of constant-resolution computation at the same resolution.

These successes are encouraging, but were achieved for one, simple, flow. They were also achieved at the cost of running two additional simulations to provide the inputs for the correction terms, and accuracy diminished significantly if changes in resolution were made too rapidly. Much work thus remains to be done to extend the theory and practice of this approach to more complex flows. In the next phase (Woodruff, 2011), the approach is successfully applied to plane channel flow turbulence, at improved accuracy and reduced cost.

## ACKNOWLEDGEMENTS

Helpful comments by R. Baurle, J. Morrison, C. Rumsey and R. Rubinstein are gratefully acknowledged.

## REFERENCES

- Brankin, R. W., Gladwell, I. and Shampine, L. F., 1992, "RKSUITE: a suite of Runge-Kutta codes for the initial value problem for ODEs," Softreport 92-S1, Department of Mathematics, Southern Methodist University, Dallas, Texas, U.S.A.
- Choi, J.-I., Edwards, J. R. and Baurle, R. A., 2009, "Compressible Boundary Layer Predictions at High Reynolds Number using Hybrid LES/RANS Methods," *AIAA J.* **47**: 2179–2193.

Davidson, L. and Billson, M., 2006, "Hybrid LES-RANS using synthesized turbulent fluctuations for forcing in the interface region," *Int. J. Heat and Fluid Flow* **27**: 1028–1042.

Germano, M., 1992, "Turbulence: the filtering approach," *J. Fluid Mech.* **238**: 325–336.

Girimaji, S. S. and Abdol-Hamid, K. S., 2005, "Partially-Averaged Navier Stokes Model for Turbulence: Implementation and Validation," AIAA 2005–502.

Hamba, F., 2009, "Log-layer mismatch and commutation error in hybrid RANS/LES simulation of channel flow," *Int. J. Heat and Fluid Flow* **30**: 20–31.

Hamba, F., 2011, "Analysis of filtered Navier-Stokes equation for hybrid RANS/LES simulation," *Physics of Fluids* **23**, 015108.

Keating, A., De Prisco, G. and Piomelli, U., 2006, "Interface conditions for hybrid RANS/LES calculations," *Int. J. Heat and Fluid Flow* **27**: 777–788.

Mansour, N. N. and Wray, A. A., 1994, "Decay of isotropic turbulence at low Reynolds number," *Physics of Fluids* **6**: 807–814.

Shebalin, J. V. and Woodruff, S. L., 1997, "Kolmogorov flow in three dimensions," *Physics of Fluids* **9**: 164–170.

Shur, M. L., Spalart, P. R., Stelets, M. Kh. and Travin, A., 2008, "A hybrid RANS-LES approach with delayed-DES and wall-modeled LES capabilities," *Int. J. Heat and Fluid Flow* **29**: 1638–1649.

Spalart, P. R., 2009, "Detached-Eddy Simulation," *Annual Review of Fluid Mechanics*, **41**: 181–202.

Speziale, C. G., 1998, "Turbulence Modeling for Time-Dependent RANS and VLES: A Review" *AIAA J.* **36**: 173–184.

Strelets, M., 2001, "Detached Eddy Simulation of Massively Separated Flows," AIAA 2001–0879.

Travin, A., Shur, M., Strelets, M. and Spalart, P., 1999, "Detached-Eddy Simulations Past a Circular Cylinder," *Flow, Turbulence and Combustion* **63**: 293–313.

Woodruff, S. L., 2011, "Merging blended turbulence models in hybrid LES-RANS computations," *NASA Technical Memorandum*, in preparation.

Woodruff, S. L., Seiner, J. M. and Hussaini, M. Y., 2000, "Grid-Size Dependence in the Large-Eddy Simulation of Kolmogorov Flow," *AIAA J.* **38**: 600–604.

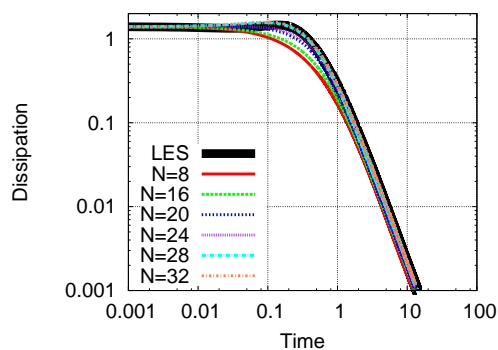


Figure 1. Target (black line) and computed dissipation. From bottom to top, resolutions  $N = 8, 16, 20, 24, 28, 32$ .

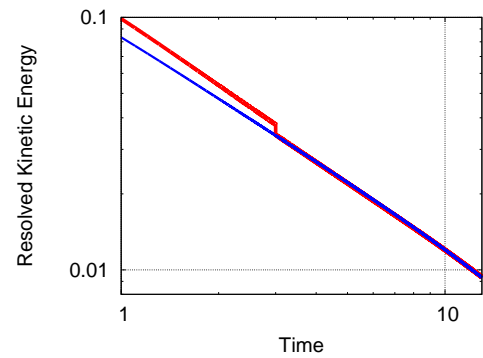


Figure 2. Kinetic energy of resolved scales: simulation beginning at  $N = 20$  and switched to  $N = 18$  at  $t = 3$ , thick red line; simulation at  $N = 18$  throughout, thin blue line.

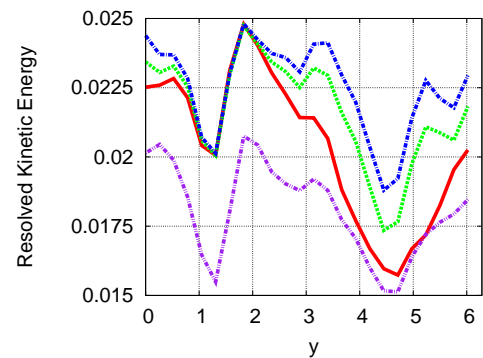


Figure 3. Plane-averaged resolved kinetic energy for spatially-varying resolution computation at  $t = 5$ : simulation with correction terms, solid red line; simulation without correction terms, dotted green line; simulation with constant  $N = 20$  resolution, dot-dashed blue line; simulation with constant  $N = 16$  resolution, double-dot-dashed purple line.

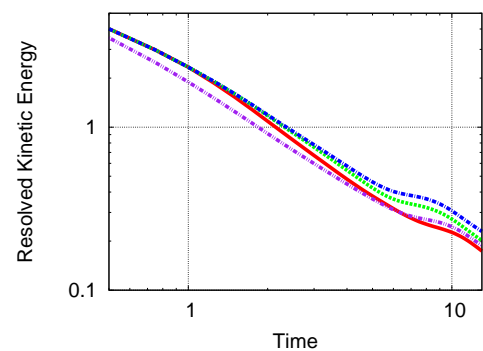


Figure 4. Time evolution of total resolved kinetic energy for spatially-varying resolution computation: same line types as Figure 3.